Electronic Supplementary Material (ESI) for Journal of Materials Chemistry B.

Standardized microgel beads as elastic cell mechanical probes

S. Girardo[1,2], N. Träber[1,3], K. Wagner[1], G. Cojoc[1], C. Herold[1], R. Goswami[2], R. Schlüßler[1], S. Abuhattum[1], A. Taubenberger[1], F. Reichel[1], D. Mokbel[1], M. Herbig[1], M. Schürmann[1], P. Müller[1], T. Heida[3], A. Jacobi[1], E. Ulbricht[1], J. Thiele[3,4], C. Werner[2,3], and J. Guck[1]

[1]Biotechnology Center, Center for Molecular and Cellular Bioengineering, Technische Universität Dresden, Tatzberg 47/49, 01307 Dresden, Germany

[2]Center for Regenerative Therapies Dresden, Center for Molecular and Cellular Bioengineering, Technische Universität Dresden, Fetscherstr. 105, 01307 Dresden, Germany

[3]Leibniz-Institut für Polymerforschung Dresden e. V., Hohe Str. 6, 01069 Dresden, Germany

[4]Faculty of Chemistry and Food Chemistry, Technische Universität Dresden, Helmholtzstr. 10, 01069 Dresden, Germany

SUPPLEMENTARY MATERIAL

Figure S1

Ammonium Krytox® surfactant, emulsion stability and surfactant analysis (A) Long-term emulsion stability test. A water-in-fluorinated oil emulsion – stabilized by the ammonium Krytox® surfactant in HFE 7500 – is stored for several days, and its stability confirmed by droplet size distribution analysis (scale bar, 50 µm). (B) FTIR spectrum of the ammonium-Krytox® surfactant and Krytox® 157 FSH as key starting material showing the conversion of Krytox® 157 FSH-carboxylic acid groups (1175 cm^{-1}) to ammonium-Krytox® carboxylate (1670 cm^{-1}).(C) Determination of the critical micellar concentration for ammonium-Krytox® by pendant droplets analysis. HFE 7500/surfactant solution is extruded from a syringe into a cuvette of double-distilled water.

Figure S2

Repeatability of bead swelling behaviour (A) Distribution of droplet diameter for different monomer concentrations (C_T) measured with bright-field microscopy. Inset: distribution of droplet diameter analyzed after production and after polymerization for a fixed total monomer concentration (C_T = 7.9%). (B) Distribution of droplet diameter for three different batches with three different monomer concentration, C_T = 7.9% (red box), C_T = 9.9% (blue box), C_T = 11.8% (green box).

Table S1

Diameter mean value for droplets ($\overline{D_{oil}}$) and beads ($\overline{D_{bead}}$), standard deviation *S.D.*, coefficient of variation *C.V.*, for droplets and beads with different monomer concentration (C_T), and the quantification of the bead swelling behavior through the calculation of the normalized volume of equilibrium of the swollen gel V_{eq} and its standard error (Δ (V_{eq})). *n* is the number of measured beads.

Figure S3

Repeatability of production process and AFM elasticity measurement (A) Young's moduli measured by AFM on three groups of five batches. Each group has a different monomer concentration, C_T = 7.9% (red box), C_T = 9.9% (blue box), C_T = 11.8% (green box).

Table S2

Young's Modulus mean value E_{mean}, standard deviation *S.D.*, and coefficient of variation *C.V.*, measured by AFM on three groups of five batches. Each group has a different monomer concentration: C_T = 7.9%, C_T = 9.9%, C_T = 11.8%. *n* is the number of measured beads.

Figure S4

Bead shape evolution in RT-DC microchannel Bead deformation (C_T = 7.9%) inside the channel depicted over time and the best exponential decay fitting curve (solid line) with τ_v = (0.12 ± 0.02) ms. The inset shows the shape evolution of a bead in the narrow channel (blue mask was applied for better visualization). It was obtained by the superposition of 7 different consecutive frames extrapolated from a video acquired at a frame rate of 2000 fps. Channel length: 300 µm, scale bar: 20 µm.

Figure S5

Flow rate optimization for RT-DC measurement, based on bead composition and effective buffer viscosity. The deformation range (0.005 - 0.05) valid for the data analysis is showed with dashed lines. (A) Histogram of PAAm beads (C_T = 7.9%) for three different flow rates and relative deformations: 0.008 µl/s (black bars) with low deformations, 0.024 µl/s (red bars) as suitable settings and 0.12 µl/s (green bars) with high deformations. (B) Histogram of PAAm beads (C_T = 7.9%) using three different measurement buffers: MC-B at 0.018 µl/s (red bars) and 68% accordance with the recommended range, MC-A at

0.024 µl/s (blue bars) and 70% accordance with the recommended range and PBS at 0.18 µl/s (black bars) and 72% accordance with the recommended range. (C) Histogram of PAAm beads for three different polymer concentrations: C_T = 7.4%, flow rate 0.012 µl/s (black bars); C_T = 7.9%, flow rate 0.024 µl/s (red bars); C_T = 8.9%, flow rate 0.04 µl/s (green bars), respectively with 83%, 96% and 96% accordance with the recommended range.

Figure S6

Comparison between AFM and RT-DC measurements. Young´s modulus obtained with AFM indentation (black boxes) and RT-DC (red boxes) for five different batches produced by using the same monomer concentration (C_T = 7.9%).

Table S3

Young's Modulus mean value E_{mean}, standard deviation *S.D.*, and coefficient of variation *C.V.*, measured by AFM and RT-DC on five batches produced with the same monomer concentration (C_T = 7.9%). *n* is the number of measured beads.

Figure S7

Consistency of RT-DC measurements Young's modulus measured by RT-DC six times, during two different days, on the same batch, having a total monomer concentration C_T = 7.9%.

Table S4

Young's Modulus mean value E_{mean}, standard deviation *S.D.*, and coefficient of variation *C.V.*, measured by RT-DC on the same batch, C_T = 7.9%, six times during two different days. *n* is the number of measured beads.

Table S5

Young's Modulus mean value E_{mean}, standard deviation *S.D.*, and coefficient of variation *C.V.*, measured by AFM on unsorted and sorted microgel beads and by RT-DC on unsorted beads. *n* is the number of measured beads.

Video S1

Pre-gel droplet production (P_{oil} =850 mbar, P_{PAAm} =700 mbar). The video was recorded at 3000 fps and showed at 30 fps.

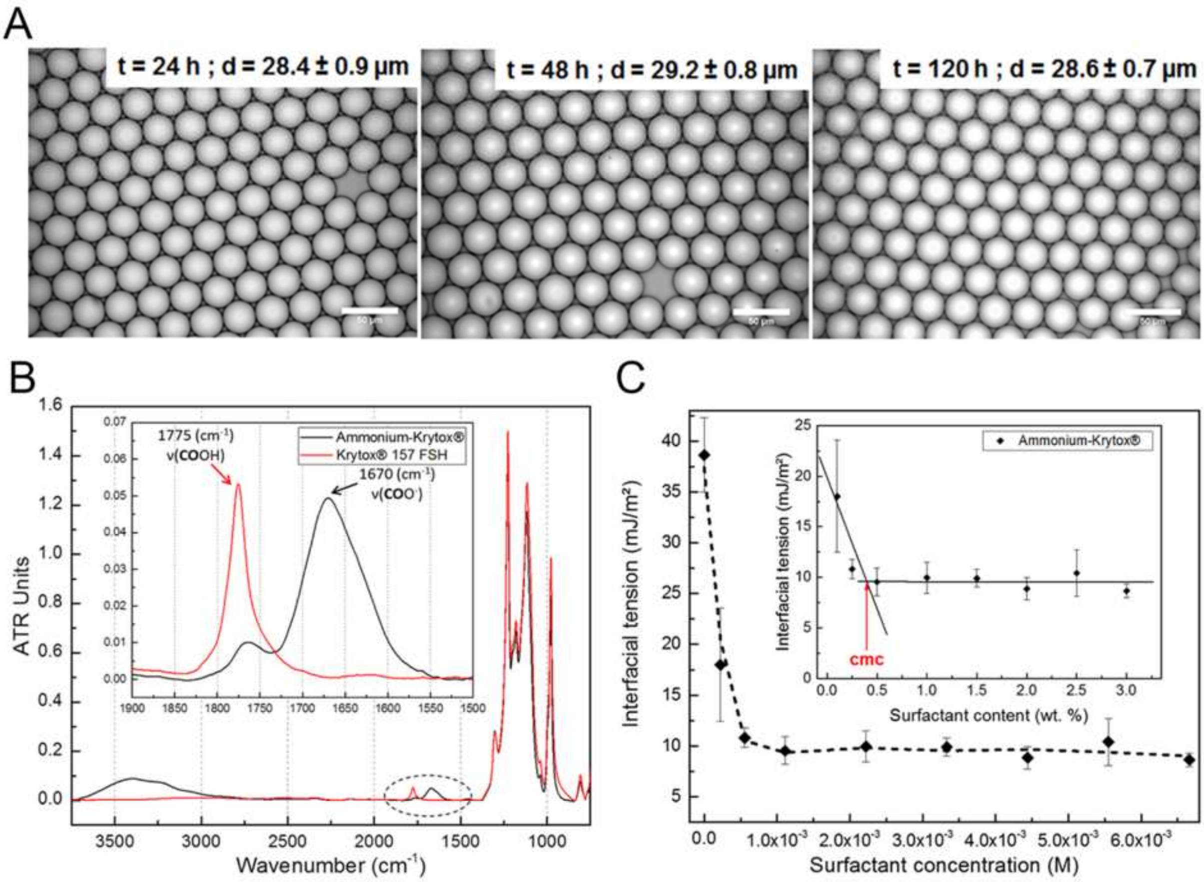

Figure S1

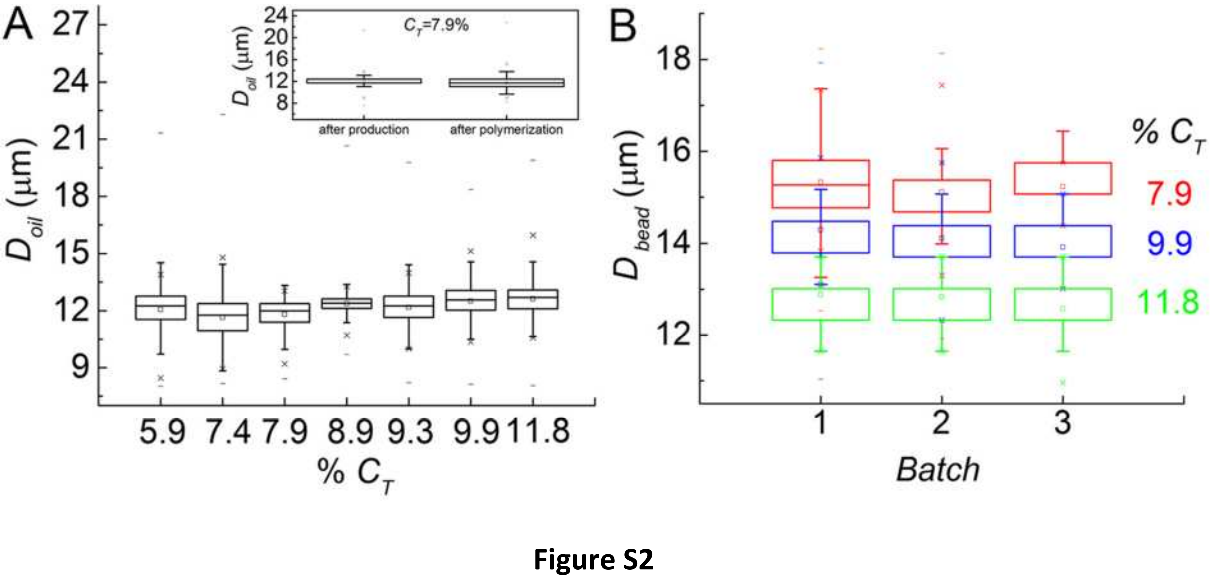

Figure S2

Size analysis											
Droplets					Beads					Swelling	
C_T (%)	n	$\overline{D_{oil}}$ (µm)	*S.D.* (µm)	*C.V.* (%)	Batch	n	$\overline{D_{bead}}$ (µm)	*S.D.* (µm)	*C.V.* (%)	V_{eq}	Δ (V_{eq})
5.9	2789	12	1	8.3		696	18	1	5.5	3.4	0.6
7.4	3618	11.6	0.9	7.7		2596	15.7	0.8	5.1	2.5	0.5
7.9	2266	11.8	0.8	6.8	1	1917	15.3	0.8	5.2	2.2	0.5
					2	1930	15.1	0.8	5.3	2.1	0.4
					3	521	15.2	0.5	3.3	1.8	0.4
8.9	2822	12.4	0.7	5.6		1790	15.0	0.6	4	1.7	0.4
9.3	3228	12.2	0.9	7.4		3469	14.6	0.4	2.7	1.7	0.4
9.9	2716	12.5	0.9	7.2	1	1914	14.3	0.6	4.2	1.5	0.4
					2	865	14.1	0.6	4.2	1.4	0.4
					3	992	13.9	0.5	3.6	1.4	0.4
11.8	2194	12.6	0.9	7.1	1	2759	12.9	0.5	3.9	1.1	0.4
					2	992	12.8	0.5	3.9	1.0	0.3
					3	811	12.6	0.5	4	1	0.3

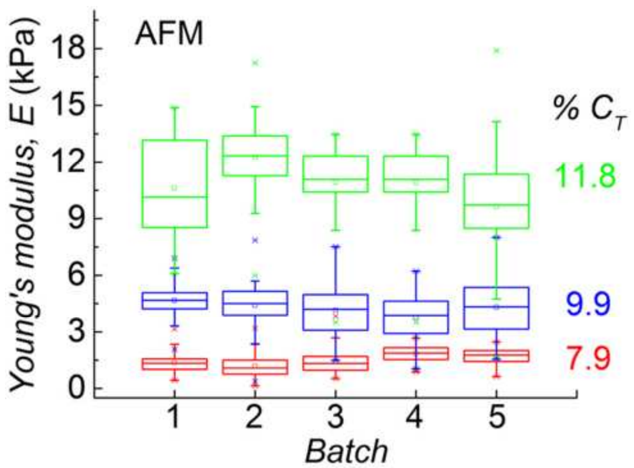

Figure S3

Repeatability of AFM elasticity measurement					
C_T (%)	Batch	*n*	E_{mean} (kPa)	*S.D.* (kPa)	*C.V.* (%)
7.9	1	73	1.4	0.5	39
	2	48	1.2	0.6	51
	3	50	1.4	0.6	45
	4	31	1.8	0.5	25
	5	40	1.7	0.4	23
9.9	1	50	4.6	0.9	20
	2	48	4.4	1.3	30
	3	42	4.1	1.4	34
	4	45	3.8	1.3	34
	5	48	4.3	1.5	35
11.8	1	32	10.6	2.6	25
	2	49	12.2	2.0	16
	3	38	10.9	1.9	18
	4	38	11.0	2.0	18
	5	48	9.6	3.3	34

Table S2

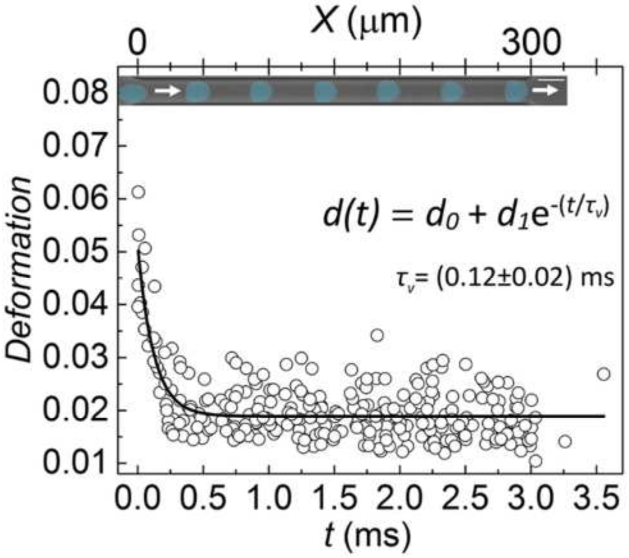

Figure S4

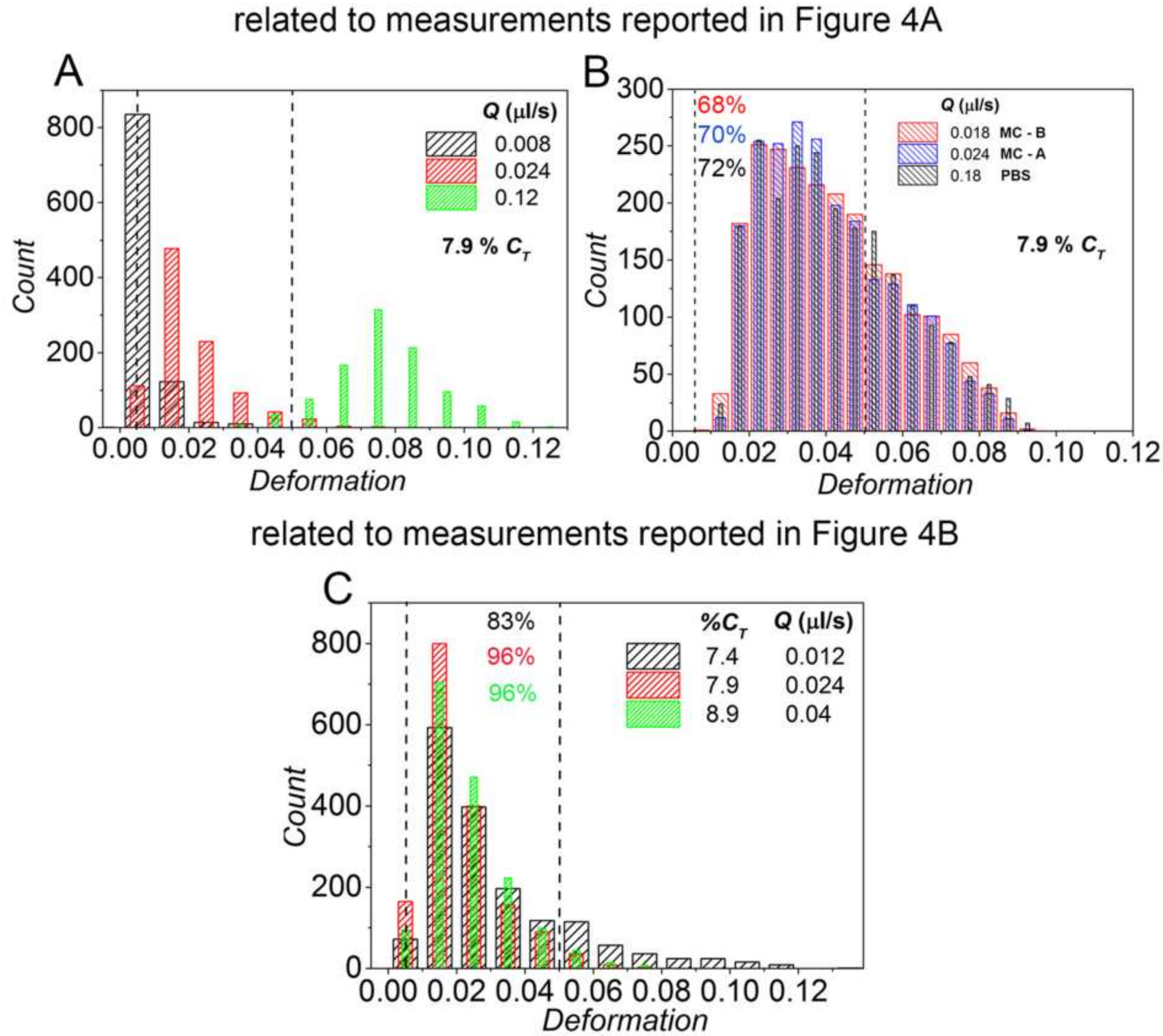

Figure S5

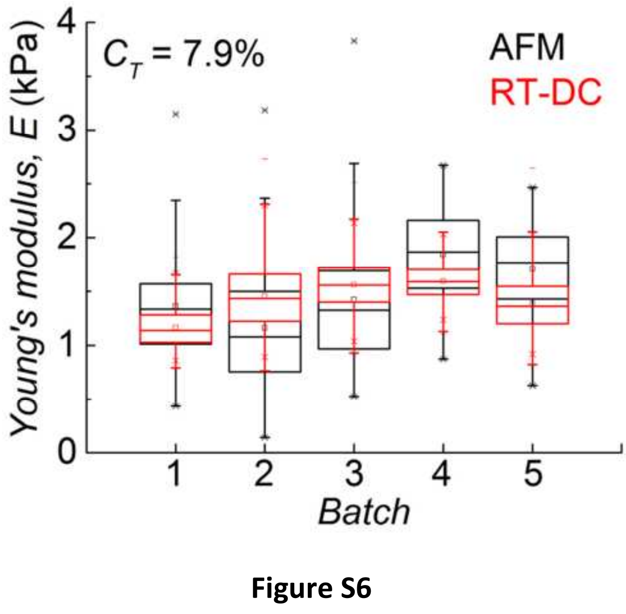

Figure S6

Different batches 7.9% C_T								
AFM					RT-DC			
Batch	***n***	**E_{mean} (kPa)**	***S.D.* (kPa)**	***C.V.* (%)**	***n***	**E_{mean} (kPa)**	***S.D.* (kPa)**	***C.V.* (%)**
1	73	1.4	0.5	39	1607	1.2	0.2	15
2	48	1.2	0.6	51	1600	1.4	0.3	21
3	50	1.4	0.6	45	1970	1.5	0.2	15
4	31	1.8	0.5	25	6534	1.6	0.2	11
5	40	1.7	0.4	23	2020	1.4	0.3	18

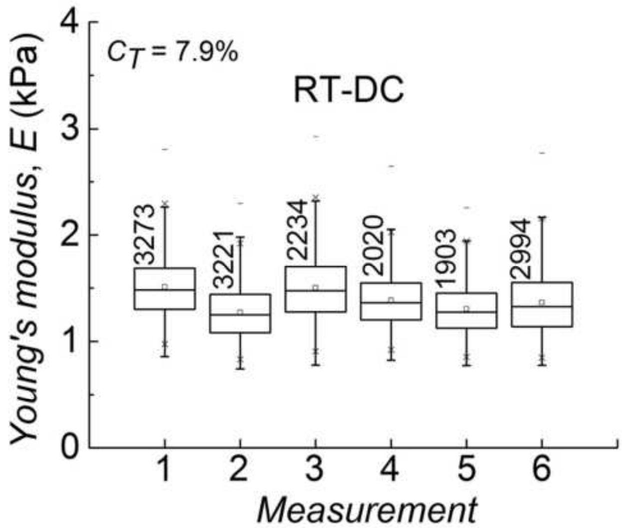

Figure S7

Same batch 7.9% C_T (RT-DC)				
Measurement	***n***	**E_{mean} (kPa)**	***S.D.* (kPa)**	***C.V.* (%)**
1	3273	1.5	0.3	19
2	3221	1.3	0.2	20
3	2234	1.5	0.3	21
4	2020	1.4	0.3	18
5	1903	1.3	0.2	18
6	2994	1.4	0.3	22

Table S4

Sorted beads					
Technique	**Sample**	***n***	**E_{mean} (kPa)**	***S.D.* (kPa)**	***C.V.* (%)**
AFM	Unsorted	50	1.2	0.5	41
	FSC low	22	0.5	0.2	37
	FSC mid	26	0.9	0.2	23
	FSC high	26	1.3	0.3	26
RT-DC	Unsorted	1402	1.1	0.2	19

Table S5